วิศวกรรมสารฉบับวิจัยและพัฒนา
Engineering Journal of Research and Development
วิศวกรรมสถานแห่งประเทศไทย ในพระบรมราชูปถัมภ์
The Engineering Institute of Thailand under H.M. The King's Patronage
ปีที่ 29 ฉบับที่ 1 มกราคม-มีนาคม 2561
Volume 29 Issue 1 January-March 2018
Received 25 May 2017
Revised 28 June 2017
Accepted 5 July 2017

CREEP DEFORMATIONS OF SALT MINE PILLARS UNDER COMPRESSED-AIR ENERGY STORAGE OPERATION

Kittisak Tengphakwaen[1], Supattra Khamrat[2], Thanittha Thongprapha[2] and Kittitep Fuenkajorn[3]
[1]Student, Geomechanics Research Unit, Suranaree University of Technology, Thailand
[2]Researcher, Geomechanics Research Unit, Suranaree University of Technology, Thailand
[3]Professor, Geomechanics Research Unit, Suranaree University of Technology, Thailand

บทคัดย่อ

ชุดการทดสอบการกดแบบวัฏจักรในสามแกนได้ถูกดำเนินการเพื่อคาดคะเนการเปลี่ยนรูปร่างเชิงเวลาของเสาค้ำยันในเหมืองเกลือที่วางแผนไว้เพื่อการกักเก็บพลังงานในรูปอากาศอัด ตัวอย่างเกลือหินถูกจัดเตรียมให้มีขนาด 54×54×108 มิลลิเมตร ความเค้นในแนวแกนและด้านข้างแบบวัฏจักรในขณะกักเก็บจะขึ้นกับความลึกของเหมือง อัตราการขุดเจาะ และความดันของอากาศที่ดันลงไป ความดันล้อมรอบที่ใช้ในการทดสอบผันแปรร้อยละ 20 (ขณะปล่อยอากาศออกมา) ถึงร้อยละ 90 (ขณะอัดอากาศลงช่องเหมือง) ของค่าความเค้นในหินที่ความลึกนั้นๆ มีการจำลองค่าความเค้นจากความลึก 250 ถึง 400 เมตร ด้วยอัตราการขุดเจาะผันแปรจากร้อยละ 30 ถึงร้อยละ 60 แต่ละตัวอย่างถูกทดสอบ 21 วัน 1 รอบวัฏจักรใช้เวลา 24 ชั่วโมง ความเครียดในสภาวะคงตัวเชิงเวลาสามารถคำนวณในรูปของความเครียดเฉือนในสามแกน ผลการทดสอบระบุว่าการกดแบบวัฏจักรจะให้ค่าความเครียดเชิงเวลาสูงกว่าการกดด้วยแรงคงที่ซึ่งเป็นจริงในทุกความลึกและอัตราการขุดเจาะ ผลการทดสอบบอกเป็นนัยว่าการเปลี่ยนรูปร่างเชิงเวลาของเสาค้ำยันในเหมืองเกลือภายใต้วัฏจักรการกดจะมีค่าสูงกว่าการเปลี่ยนรูปร่างภายใต้การกดแบบแรงคงที่ พลังงานความเครียดเบี่ยงเบนได้นำมาใช้เพื่อการคาดคะเนกำลังของเสาค้ำยันเกลือภายใต้การกดแบบวัฏจักร ผลที่ได้ระบุว่าภายใต้การกักเก็บพลังงานในรูปอากาศอัดอายุการใช้งานของเสาค้ำยันในเหมืองเกลือจะลดลงเมื่ออัตราการขุดเจาะและความลึกของเหมืองเพิ่มขึ้น

ABSTRACT

Series of triaxial cyclic loading tests have been performed to predict the time-dependent deformation of supported pillars in abandoned salt mines planned for a compressed-air energy storage operation. The salt specimens are prepared to obtain rectangular prisms with nominal dimensions of 54×54×108 mm. The applied axial and lateral cyclic stresses depend on mining depths, extraction ratios and injection pressures. The confining pressures vary from 20% (withdrawal) to 90% (injection) of the in-situ stresses. The stress conditions are calculated for the depths from 250 to 400 m with extraction ratios ranging from 30 to 60%. All tests are performed up to 21 days. Each cycle takes 24 hours. The steady-state creep strains are calculated in terms of the octahedral shear strains as a function of time. The cyclic loading induces a higher creep strain than that of the static loading for all depths and extraction ratios, suggesting that the time-dependent deformations of salt pillars are greater under cyclic loading than under static loading. The distortional strain energy at failure is used to predict the time-dependent strengths of the

salt pillars. The results suggest that under storage operation the duration under stable condition of the salt pillars decreases with increasing extraction ratios and mining depths.

KEYWORDS: Time-dependency, Creep, Strain Energy Density, Potential Creep Law, Extraction Ratio

1. Introduction

The effect of cyclic loading on the elasticity and strengths of geologic materials has long been recognized [1-2]. A common goal of the previous studies is to determine the fatigue strength of the materials. It has been found that loading cycles can reduce the material strength and elasticity, depending on the loading amplitude and the maximum applied load in each cycle [3-6]. Rare investigation has however been made to identify the cyclic loading effect on the time-dependent properties and behavior of soft and creeping materials, such as salt, particularly within the steady-state phase. Such knowledge is important for the compressed-air energy storage in an abandoned salt mine. The salt pillars will subject to cycles of vertical and lateral loading and unloading. As a result the creep deformation of the salt pillars could be different from that when they are under static loading during excavation.

The objective of this study is to determine the time-dependent deformations of rock salt under triaxial cyclic loading. A total of 12 specimens has been tested for up to 21 days. The creep strains are monitored and used as an indicator of the effect of cyclic loading on the salt specimens. The test is performed to simulate the time-dependent deformation of pillars in abandoned salt mines during air injection-withdrawal condition. Potential creep law is used to describe the time-dependent deformations of rock salt. Strain energy density criterion from related studied are used to predict the time-dependent strengths of the pillars under various depths and extraction ratios.

2. Sample Preparation

Salt specimens are collected from an underground salt mine in the northeast of Thailand. They belong to the Lower member of the Maha Sarakham formation. The specimens are prepared to obtain rectangular prisms with nominal dimensions of 54×54×108 mm^3. The specimen main axis is normal to the bedding planes. The average density is 2.19 ± 0.03 g/cm^3.

3. Test Method

A polyaxial load frame [7] has been used to apply axial and lateral stresses to the salt specimens. Neoprene sheets are placed at the interfaces between loading platens and rock surfaces to minimize the friction. To simulate the stress conditions under storage operation the tributary area concept is used. The axial stress (σ_1) is applied on the specimens for the extraction ratios (e) of 30, 40 and 60%. The maximum and minimum lateral stresses used during cyclic loading are defined as 90% and 20% of the in-situ stresses (at the mine roof) equivalent to the depths of 250, 300, 350 and 400 m. The axial stresses can be obtained as follows:

$$\sigma_1 = \sigma_p - 90\% \, \sigma_v \cdot e \qquad \text{during injection} \qquad (1)$$

$\sigma_1 = \sigma_p - 20\% \sigma_v \cdot e$ during withdrawal (2)

The lateral stresses (σ_3) can be determined by:

$\sigma_3 = 90\% \sigma_v$ during injection (3)

$\sigma_3 = 20\% \sigma_v$ during withdrawal (4)

$\sigma_v = \rho H$ (5)

where $\sigma_p = [\sigma_v / (1 - e)] \times 100$, σ_v is in-situ stress, H is mine depth, and ρ is in-situ stress gradient of overburden (approximated here as 0.021 MPa/m). Figure 1 shows the stress paths during excavation and storage operations. A constant axial stress (σ_1) is first applied to the rock specimens for 12 hours before testing. This is to ensure that the salt deformation has gone into the steady-state creep phase. Table 1 gives the test variables for the axial and lateral stress cycles corresponding to the depths and extraction ratios above. Each cyclic takes 24 hours. The test period is 21 days for each specimen. The vertical and lateral deformations are monitored using displacement dial gages. A total of 12 specimens have been tested.

4. Test Results

Figure 2 shows the axial (ε_{ax}) and lateral (ε_{lat}) strain-time curves of salt specimen at each depth and extraction. The curves show the instantaneous, transient and steady-state creep phases. The salt specimens deform without failure up to 21 days. The strains increase with increasing extraction ratios, particularly under great depths. The effects of cyclic loading can be observed for both axial and lateral strains during steady-state creep phase. The strain amplitudes tends to be consistent for each extraction ratio and depth. For each loading cycle small instantaneous and transient strains can be measured during loading and unloading, suggesting that even under the steady-state deformation the salt still exhibits elastic and visco-elastic behavior.

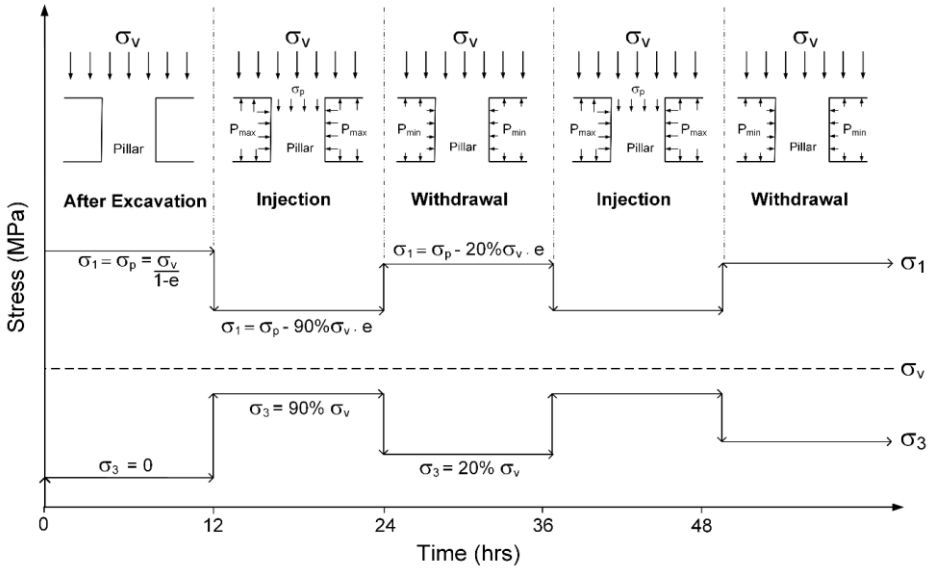

Figure 1 Cyclic stress paths as a function of time

Table 1 Test variables

Mine Parameters					Storage Parameters		Octahedral Shear Stresses in Pillars
					Injection	Withdrawal	Withdrawal
Depth (m)	σ_v (MPa)	e (%)	σ_p (MPa)	σ_m (MPa)	P_{max} (90%σ_v) (MPa)	P_{min} (20%σ_v) (MPa)	τ_o (MPa)
250	5.3	30	7.5	3.63	4.7	1.7	2.73
		40	8.8	4.05			3.32
		60	13.1	5.51			5.39
300	6.3	30	9.0	4.13	5.7	1.7	3.44
		40	10.5	4.63			4.15
		60	15.8	6.38			6.62
350	7.4	30	10.5	4.63	6.6	1.7	4.15
		40	12.3	5.22			4.97
		60	18.4	7.26			7.86
400	8.4	30	12.0	5.13	7.6	1.7	4.86
		40	14.0	5.80			5.80
		60	21.0	8.13			9.10

5. Calibration of Creep Parameters

To consider both axial and lateral creep strains, the octahedral shear stresses and strains during cyclic loading are determined using the following relations [8]:

$$\tau_o = \left(\sqrt{2}/3\right)\cdot\left(\sigma_{1,\text{with}} - \sigma_{3,\text{with}}\right) \tag{6}$$

$$\gamma_o = (1/3)\cdot[(\varepsilon_1-\varepsilon_2)^2 + (\varepsilon_1-\varepsilon_3)^2 + (\varepsilon_2-\varepsilon_3)^2]^{1/2} \tag{7}$$

where τ_o are maximum octahedral shear stresses calculated under withdrawal conditions (Table 1), $\sigma_{1,\text{with}}$ and $\sigma_{3,\text{with}}$ are the major and minor principal stresses, during loading (withdrawal), γ_o is the octahedral shear strain, and ε_1, ε_2 and ε_3 are the measured major, intermediate and minor principal strains. The octahedral shear strains are plotted as a function of time in Figure 3. The test results show that the salt creep increases with time and tend to be relatively constant in the steady-state creep phase.

The total shear strain in salt specimens can be divided into two parts, elastic strain (linear and recoverable strain) and plastic creep strain (time-dependent and nonrecoverable strain):

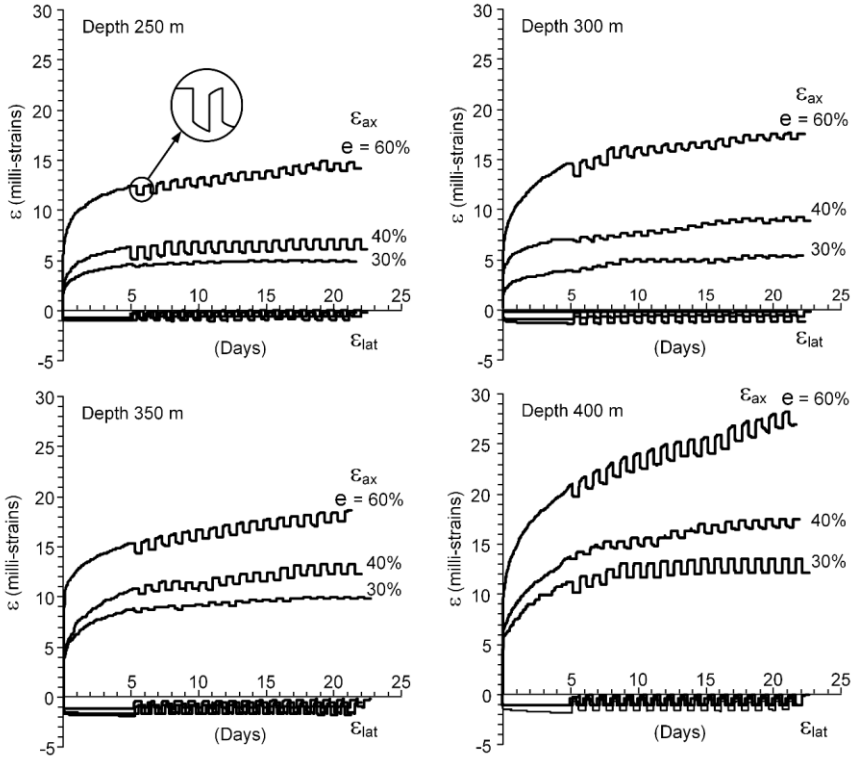

Figure 2 Axial (ε_{ax}) and lateral (ε_{lat}) strain-time curves under cyclic loading for various depths and extraction ratio

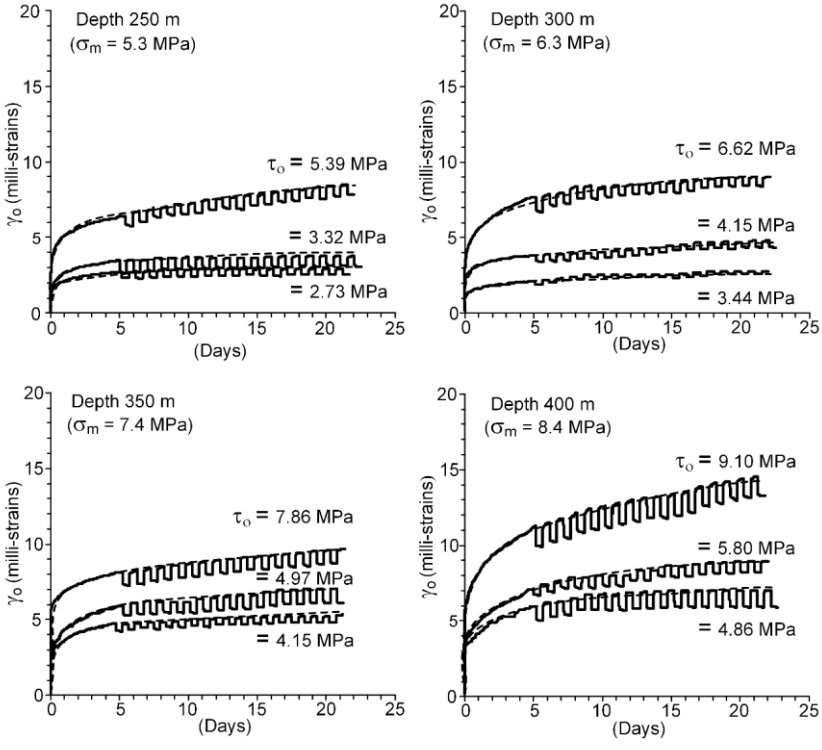

Figure 3 Octahedral shear strains as a function of time for various octahedral shear stresses (solid lines) and potential law curves fitting (dash lines)

$$[\gamma_o^T] = [\gamma_o^e] + [\gamma_o^c] \tag{8}$$

where $[\gamma^T]$, $[\gamma^e]$ and $[\gamma^c]$ are three-dimensional vectors of total, elastic and time-dependent strains.

The elastic strain from the test results can be obtained from the constant octahedral shear stress and shear modulus (G) which can be written as:

$$\gamma_o^e = \tau_o / 2G \tag{9}$$

The potential creep law are used to present the creep behavior of salt in terms of the octahedral shear stress and octahedral shear strain as a function of time for the steady-state creep phase.

$$\gamma_o^c = \kappa \tau_o^{\beta} t^{\gamma} \tag{10}$$

where κ, β and γ are material parameters. Substituting equations (9) and (10) into (8) the total octahedral shear strain can be presented as a function of time and octahedral shear stress and plastic creep strain:

$$\gamma_o^T = (\tau_o/2G) + (\kappa \tau_o^{\beta} t^{\gamma}) \quad (11)$$

The shear modulus can be obtained from relatively quick loading as those performed by Luangthip et al. [9] on the same rock salt. They define G as 7.84 GPa

Regression analyses on the octahedral shear strain-time curves based using the SPSS statistical software [10] are performed to determine the creep parameters for each specimen. Figure 3 shows the calibration results of the steady-state creep phase by using equation (11). They are presented by dash line in the figure. The calibrated parameters for the cyclic test results are κ = 5.36 1/MPa·s, β = 1.26 and γ = 0.16 with R^2 >0.9. Table 2 compares these parameters with those of the static loading test by Wilalak [11]. The results indicate that the parameter κ obtained from cyclic loading test is higher than that of the static loading test, suggesting that the salt tends to be softer and more sensitive to time when it is under cyclic loading.

6. Time-dependent Strength of Pillars

The time-dependent deformation of rock salt under cyclic loading is an important factor for the planning of compressed-air energy storage operation. This is mainly to ensure that the pillar remains mechanically stable during operation. The strain energy density principle is applied here to describe the salt pillar stability under different extraction ratios and depths. The calculation are made for the depths from 250 to 400 m with extraction ratios from 30% to 60%. The distortional strain energy can be calculated from the octahedral shear stress and strain using the following relation:

$$W_{d,p} = (3/2) \cdot \tau_o \cdot \gamma_o^T \quad (12)$$

Table 2 Creep parameter of static and cyclic loading

Creep Parameters	Static Loading (from Wilalak [11])	Cyclic Loading
κ ($\times 10^{-9}$/ MPa·s)	2.97	5.36
β	1.37	1.26
γ	0.19	0.16

where τ_o is maximum octahedral shear stress depending on extraction ratios and depths and γ_o^T is the octahedral shear strain as a function of time.

In order to describe the increase of the pillar deformation (strain) with time under the triaxial cyclic loading condition, the potential creep law in equation (11) can be used. By substituting the material parameters G, κ, β and γ in to equation (11) a series of octahedral shear strains time curves for salt pillars under various depths and extraction ratios can be developed. The pillar strains and their corresponding time at which the failure occurs can be determined by comparing the distortional strain

energy obtained here with the strain energy criterion of rock salt at failure developed by Junthong [12], as shown in Figure 4. The factor of safety (FS) can be determined with relation to time, depth and extraction ratio of pillars.

$$FS = W_d/W_{d,p} \quad (13)$$

where W_d is the distortional strain energy criterion given by Junthong [12], $W_{d,p}$ is the distortional strain energy calculated from the test results by substituting equations (11) into (12):

$$W_{d,p} = [(3/2\cdot \tau_o)\cdot[(\tau_o / 2G)] + (\kappa \tau_o^{\beta})t^{\gamma}]] \quad (14)$$

The results suggest that the duration under stable condition (FS > 1.0) decreases with increasing extraction ratios and mining depths. Figure 5 gives an example of the factor of safety calculation for the storage operation life of 20 years. The diagram compares the FS obtained under cyclic loading with that of the static loading by using the two sets of creep parameters given in Table 2.

7. Discussions and Conclusions

The effects of cyclic loading are determined from the salt specimens obtained from the Maha Sarakham formation. A polyaxial load frame applies axial and lateral stresses to the salt specimens. The tributary area concept is used to determine the axial stress. The lateral stresses depend on injection and withdrawal pressures. The calculations are made for the depths from 250 to 400 m, with extraction ratios ranging from 30 to 60%. The results show that the axial strains increase with increasing extraction ratios, particularly under high in-situ stresses. Good correlation coefficients ($R^2 > 0.9$) are obtained from the regression analysis using the potential equation. The stress constant κ obtained from the cyclic loading test is higher than that of the static loading. This means that the pillars can deform more quickly under cyclic loading than under static loading. The diagram in

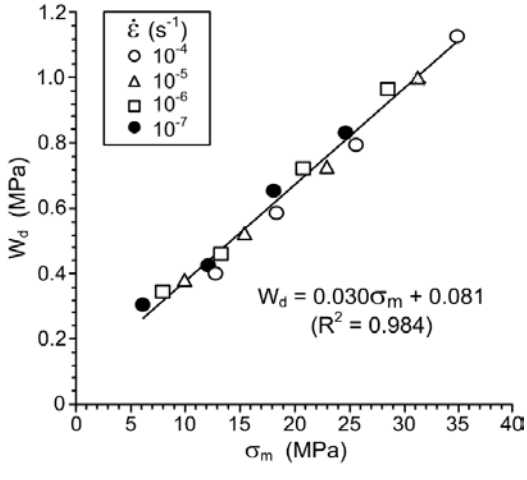

Figure 4 Distortional strain energy (W_d) at failure as a function mean stress (σ_m) [12]

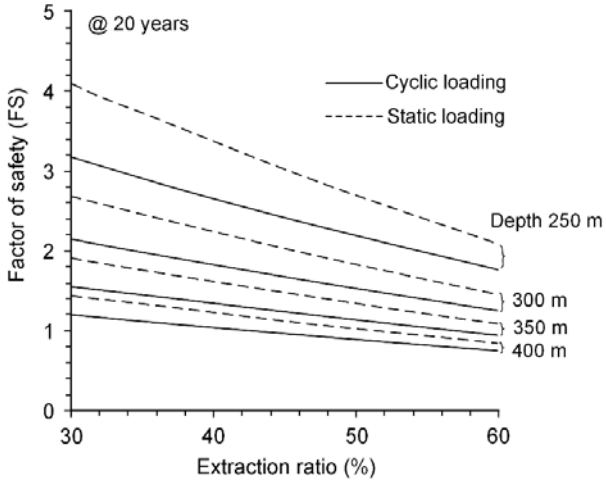

Figure 5 Factors of safety as s function of extraction ratio for four mine depths, comparing static (dash lines) with cyclic (solid lines) loading conditions at year 20 of operation

Figure 5 can be used as a guideline for the compressed-air energy storage planning and for the performance assessment of the rock salt formations in the northeast of Thailand. The pillar deformation may be sensitive to the types of creep model. Application of different constitutive models for the rock salt may result in different predictions of the pillar deformations and failure.

Acknowledgements

This study is funded by Suranaree University of Technology and by the Higher Education Promotion and National Research University of Thailand. Permission to publish this paper is gratefully acknowledged.

References

[1] Allemandou, X. and Dusseault, M. B. Procedures for cyclic creep testing of salt rock, results and discussions. *Proceeding of the Third Conference on the Mechanical Behavior of Salt*, Clausthal-Zellerfeld, 14-16 September 1993, pp. 207-218.

[2] Bagde, M. N. and Petros, V. Fatigue properties of intact sandstone samples subjected to dynamic uniaxial cyclical loading. *International Journal of Rock Mechanics and Mining Sciences*, 2005, 42 (2), pp. 237-250.

[3] Zhenyu, T. and Haihong, M. An experimental study and analysis of the behaviour of rock under cyclic loading. *International Journal of Rock Mechanics and Mining Sciences*, 1990, 27 (1), pp. 51-56.

[4] Ray, S. K. *et al.* Effect of cyclic loading and strain rate on the mechanical behaviour of sandstone. *International Journal of Rock Mechanics and Mining Sciences*, 1999, 36 (4), pp. 543-549.

[5] Kodama, J. *et al.* Estimate of the fatigue strength of granite subjected to long-period cyclic loading. *Shigen-to-Sozai*, 2000, 116, pp. 111-118.

[6] Fuenkajorn, K. and Phueakphum, D. Effects of cyclic loading on mechanical properties of Maha Sarakham salt. *Engineering Geology*, 2010, 112, pp. 43-52.

[7] Fuenkajorn, K. *et al.* Effects of loading rate on strength and deformability of Maha Sarakham salt. *Engineering Geology*, 2012, 135-136, pp. 10-23.

[8] Jaeger, J. C. *et al. Fundamentals of rock mechanics*. Chapman and Hall: London, 2007.

[9] Luangthip, A. *et al.* Effects of carnallite contents on stability and extraction ratio of potash Mine. In: *9th Asian Rock Mechanics Symposium*, Bali, Indonesia, 18-20 October 2016.

[10] Wendai, L. *Regression analysis, linear regression and profit regression, In 13 chapters, SPSS for Windows: statistical analysis*. Beijing: Publishing House of Electronics Industry, 2000.

[11] Wilalak, N. *Time-dependent behavior of Maha Sarakham salt as affected by carnallite content*. Master Degree thesis, Suranaree University of Technology, 2016.

[12] Junthong, P. *Effect of strain rate on strength and deformability of Maha Sarakham salt*. Master Degree thesis, Suranaree University of Technology, 2016.